Engineering Transactions, **73**(4): 617–633, 2025, https://doi.org/10.24423/engtrans.3489.2025
Institute of Fundamental Technological Research Polish Academy of Sciences (IPPT PAN)
Université de Lorraine • Poznan University of Technology

Research Paper

Analysis of the Braking Process for Curvilinear Motion of Vehicle

Piotr FUNDOWICZ, Hubert SAR, Mateusz BRUKALSKI*, Michał ABRAMOWSKI

Institute of Vehicles and Construction Machinery Engineering
Warsaw University of Technology
Warsaw, Poland

*Corresponding Author e-mail: mateusz.brukalski@pw.edu.pl

Road incident reconstruction frequently includes the possibility of avoiding a collision. To perform such analysis, it is necessary to compare the available distance with the minimum braking distance. Therefore, to avoid a collision, the braking distance must be shorter than the available distance. The braking distance depends on parameters such as tyre-to-road adhesion coefficient, the initial velocity of a vehicle, the driver's reaction time and the time needed to reach full braking force. However, the problem is that, in practice, none of these values are known during traffic incident reconstruction. As a result, the estimated vehicle velocity is uncertain. This is due to the method used to reconstruct a road incident (and the errors in the evidence data). The tyre-to-road adhesion coefficient depends on many factors and can be estimated with limited accuracy, usually ± 0.1. The uncertainty of the estimate is approximately $\pm 15\%$. The reaction time of a specific driver under the conditions present during a road incident is not precisely known. Therefore, an average value for most drivers is taken into account. It is assumed that a healthy driver's reaction time should not exceed this value, and a longer reaction time is associated with incorrect driving behavior. The time taken to reach full braking force in a real situation is also unknown. Usually, average values are taken from the literature, without the analysis of a technical condition of a vehicle. This article considers the mechanics of vehicle braking, taking into account the action of lateral forces on this vehicle while considering a curved track. The maximum deceleration during braking is determined analytically, and a condition is formulated to indicate whether it is justified to use an advanced computational model instead of the basic one described in the literature. The analysis includes some dimensionless parameters describing the position of the center of gravity, tangential forces between the tyre and the road, the intensity of turning and braking, suspension characteristics, and asymmetrical mass distribution. This dimensionless approach may be useful for applying the presented analysis of braking on the road arc in accident reconstruction, especially when comparative analysis is recommended.

Keywords: active safety; braking on the road arc; braking force; driver reaction time; intensity of turning.

1. Introduction

The process of vehicle braking is essential when analyzing active safety of vehicles, especially in the reconstruction of traffic incidents. The course of braking maneuver depends on many factors, including driver reaction time, as discussed in [1–3]. Specifically, in [1] the authors analyzed different scenarios of the maneuvers on a road, with the application of a model designed to simulate obstacle avoidance and vehicle braking. The main factors in this model were: the coefficients of adhesion in both longitudinal and lateral directions, and the braking reaction time [1]. Modern vehicles are equipped with driver-assistance systems that may help prevent traffic incidents. One of such systems is automatic emergency braking (AEB), which was the subject of research in [4]. The authors of [4] presented a rapid verification method for the AEB control algorithm, which was based on a verification system integrating software-in-the-loop (SIL) and hardware-in-the-loop (HIL) for a passenger car. Article [5] also investigated AEB systems and highlighted their positive impact, reporting a significant reduction in accidents in both urban and extra-urban areas.

Another paper, [6], discussed the influence of vehicle-to-everything (V2X) communication on driver reaction times and behavior. Additionally, in [6], the reaction times regarding separately a driver response to steering wheel and brake pedal inputs were analyzed. It was concluded that an absence of a warning signal does not increase a driver distraction. In [7], an approach to risk assessment for autonomous vehicles moving on roundabouts was presented. The authors addressed here sudden braking and maximum braking capability. The next article in which the authors discuss controlling the trajectory of autonomous vehicle under various curved road conditions is the work presented in [8]. The braking process of vehicle depends not only on vehicle and driver characteristics but also on the anti-skid properties of the road surface, as explored in [9–12]. Additionally, the feature of emergency braking combined with obstacle avoidance at high velocities, including active steering, was examined in [13].

Papers [14, 15] showed the application of the so-called bicycle model of a vehicle for simulating vehicle motion. The authors of [14] presented a curvilinear motion model for a truck, where dynamic changes in brake force distribution, tire normal load, and both longitudinal and lateral adhesion during braking were considered. The model also examined non-steady-state response of the truck and the potential for skidding. The authors performed their analysis for the truck moving on horizontal curves.

The vehicle motion was investigated in the study by Zhu and Hong [15]. The authors applied here a simplified bicycle model of a vehicle together with an investigation of the effects of vehicle dynamics stiffness. They decided to include this approach for the needs of path-tracking control for autonomous vehicles.

Article [16] showed the strategy for an adaptive cruise control (ACC) system for intelligent vehicles based on hierarchical control. The authors applied here a brake/throttle opening switching model, a brake control inverse model, and a throttle opening inverse model for the needs of regulating the ACC by obtaining the desired throttle opening and braking pressure.

In [17] authors demonstrated the use of SIL and HIL testing methods in an automated test environment to enhance software development and testing processes, among others, for the ABS functioning.

The braking process and its participation in an electric vehicle motion, including the number of braking events, stops, acceleration time, and regenerative braking were extensively described in [18]. The real driving scenarios included varying traffic densities, speed limits, and elevation profiles were presented.

Article [19] presented an optimized control algorithm for AEB, including the time to collision (TTC) to improve driving comfort. In [19], the analyzed braking scenarios included two different types of following vehicles – a passenger vehicle and a commercial vehicle.

The problem of investigating full vehicle dynamics for the purpose of developing stability control system was presented in [20], where a 12 degree-of-freedom (DOF) vehicle model (also including a driver model and a linear tyre model) was used. The authors of [20] based their analysis on two maneuvers – the J-turn and the single lane change.

The braking process is especially important in the motion of trucks, which is the subject of studies [21, 22]. The impact of an emergency braking scenario on the structural strength of a truck tractor frame is examined in [21]. D'Alembert's principle as well as a semi-trailer and a truck unit frame calculation scheme were applied in [21] for emergency braking during straight-line driving. In [22], it was analyzed how selected parameters of a tractor-semitrailer set influenced the braking process. The study discussed the effectiveness of braking process under changeable operating conditions [22].

A serious challenge is evaluating vehicle braking on a curved path. In most cases, the stopping distance on a curve is longer than on a straight section of road. In many cases, however, the difference in the length of the stopping distance between straight and curved paths may be small, comparable to the estimation uncertainty, which results from the uncertainty of parameter estimation used in the calculations. This study analyzes the braking process of a vehicle in curvilinear motion – that is, braking on a curved road modeled as a circular road arc with a constant radius. The forces acting on individual wheels of a vehicle during braking, considering the simultaneous effect of lateral forces resulting from curvilinear motion, acting on a vehicle, are studied. The described model, hereinafter referred to as advanced computational model, is compared with a simple computational model, commonly found in the litera-

ture (see, e.g., [23]). Based on this comparison, the conclusions are formulated, which indicate the need to use an advanced computational model in the analysis of traffic incidents.

2. The stopping distance and the braking distance

The review of the literature presented in the first section showed the importance of driver reaction times [1–3], the role of automatic emergency brake [4, 5] as well as active steering when avoiding an obstacle, as mentioned in [13].

The authors decided to present the problem of braking on a curved path in a way that is useful for traffic incidents analysis. This is achieved through a dimensionless approach to some parameters characterizing the vehicle, which will be presented in further sections of this paper.

Returning to the substantive part of this work, the vehicle stopping distance is analyzed using two methods: a simplified method, in which the vehicle is represented as a material point with negligible dimensions, and an advanced model, in which the forces acting on each individual wheel are analyzed. The first model is considered in many analyses, e.g., [23, 24]. It allows for determining the vehicle minimum stopping distance assuming an ideal braking system and ideal traffic conditions. A similar approach is also used, e.g., in [25], where the braking process of a single wheel is analyzed using a quarter-car dynamics model, and the calculation results are considered to represent the entire vehicle. In this model, it is assumed that the pressure of the analyzed wheel is equal to one quarter of the vehicle's weight. While in static conditions this may be an acceptable simplification, it cannot be accepted when braking with high intensity (which corresponds to the minimum braking distance), and especially when discussing the vehicle curvilinear motion.

The stopping distance S_Z is the sum of the driver's reaction distance S_R, the distance during which the braking force is increasing S_N, and the distance when the braking force is stabilized S_H – also known as the braking distance [26, 27]. Of course, the distance of driver's reaction S_R depends on the driver's reaction time:

$$S_Z = S_R + S_N + S_H. \tag{2.1}$$

In the majority of analyzed cases, the time during which the braking force increases (t_N) is much shorter compared to the total braking time. So, there can be assumed a simplification, which takes zero value during the first half of t_N and reaches a steady-state value during the second half. In practice, we use the following formula for computing (estimating) the braking distance:

$$S_Z = v_0 \cdot \left(t_R + \frac{1}{2} t_N \right) + S_H. \tag{2.2}$$

It can be stated that the results of the calculations using Eq. (2.2) do not differ from the results obtained by performing more accurate calculations.

Investigations show that the deceleration during intensive braking on a straight road is constant. In real-world cases, the braking force is slightly higher during the initial and final phases of braking than its value in steady-state conditions, but this has small influence on the length of the braking distance. So, for computing the braking distance the following well-known equation is presented:

$$S_H = \frac{v_0^2}{2 \cdot g \cdot \mu}, \tag{2.3}$$

where v_0 is the initial velocity of the vehicle [m/s], g is the gravity coefficient, $g = 9.81$ m/s^2, and μ is the coefficient of adhesion (dimensionless).

Note that this is the smallest value of braking distance.

When a vehicle is moving on a curved road, the lateral forces acting on the vehicle are balanced by the lateral forces between the tyres and the road surface. Since the total tangential force between the wheels and the road surface is the vector sum of the braking force and the lateral force, the maximum braking force when driving around a curve is lower than when the vehicle is braking on a straight road.

3. Simple computational model

An example of braking distance calculations on the road arc is shown in [28]. The braking vehicle is considered as a material point moving on a plane. It is assumed that each wheel is working under the same conditions. Although there are advanced, non-linear methods to describe the forces of adhesion, e.g., [29], the force between the tyre and the road surface is often well described by linear equations. Therefore, by analyzing the forces in both lateral and longitudinal directions, the following equations can be written, in which the forces acting on all wheels of the vehicle are summed [30, 31]:

$$m \cdot g \cdot \gamma_x = \sum Z \cdot \mu_x, \tag{3.1}$$

$$m \cdot g \cdot \gamma_y = \sum Z \cdot \mu_y, \tag{3.2}$$

where the summation refers to all wheels of the vehicle, m is the mass of the vehicle [kg], Z is the vertical forces between the tyres and the pavement [N], μ_x, μ_y are the unitary (dimensionless) forces between the tyres and the pavement in the longitudinal and lateral directions, i.e., the ratio of horizontal forces to vertical forces, γ_x is the braking intensity coefficient defined as the ratio of vehicle deceleration to gravitational acceleration (a_x/g) (dimensionless), and γ_y is

the turning intensity coefficient defined as the ratio of lateral acceleration to gravitational acceleration (a_y/g), and it is dimensionless.

The sum of the normal forces between the tyres and the road surface is equal to the weight of the vehicle:

$$\sum Z = m \cdot g. \tag{3.3}$$

The unitary forces in the longitudinal and lateral directions have to satisfy the following relationship:

$$\left(\frac{\mu_x}{\mu_{\mathrm{MX}}}\right)^2 + \left(\frac{\mu_y}{\mu_{\mathrm{MY}}}\right)^2 - 1 \leq 0, \tag{3.4}$$

where μ_{MX}, μ_{MY} are the coefficients of adhesion in the longitudinal and lateral directions, respectively (dimensionless).

Using Eqs. (2.3), (3.1), and (3.2), we can compute the maximum value of the intensity of braking without the loss of stability of motion:

$$\gamma_{x\,\max} = \mu_{\mathrm{MX}} \cdot \sqrt{1 - \left(\frac{\gamma_y}{\mu_{\mathrm{MY}}}\right)^2}, \tag{3.5}$$

and in the next step, the maximum value of deceleration can be calculated as:

$$a_H = \gamma_{x\,\max} \cdot g. \tag{3.6}$$

If there are no data about the difference between the values of the coefficients of adhesion in the longitudinal and lateral directions, we can assume that these coefficients have the same value. In this case, the deceleration can be expressed as follows:

$$a_H = g \cdot \sqrt{\mu^2 - \gamma_y^2}. \tag{3.7}$$

The intensity of turning (lateral acceleration) depends on the curvature of the road (described by the radius R) and the velocity of the vehicle's center of mass v; thus, the maximum deceleration decreases as the velocity increases, and it can be calculated using Eq. (3.8):

$$a_H(v) = \sqrt{g^2 \cdot \mu^2 - \frac{v^4}{R^2}}. \tag{3.8}$$

When $a_H(v)$ from Eq. (3.8) is known, we can compute the braking distance by numerical integration according to the scheme shown in Fig. 1. This scheme corresponds to the integration:

$$v(t) = \int_0^t a_H \,\mathrm{d}t, \qquad S(t) = \int_0^t v(t) \,\mathrm{d}t. \tag{3.9}$$

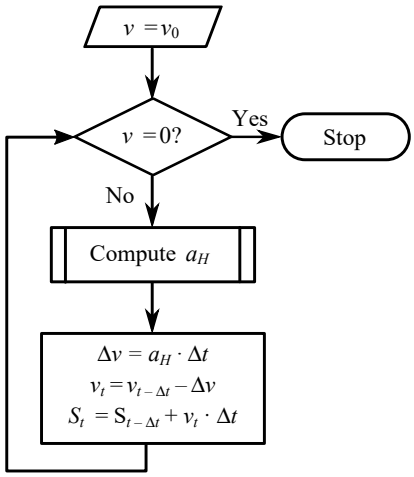

FIG. 1. Algorithm for computing the braking distance.

4. Advanced computational model

For the needs of a more precise description of braking, each wheel of the vehicle should be considered separately. The model described applies to vehicles without ABS or to vehicles with ABS before its activation.

When a vehicle is braking with an intensity γ_x and simultaneously turning with an intensity γ_y, the normal forces between the tyres and the road surface are (where "+" for the right wheels, "−" for the left wheels):

$$Z_{1R,1L} = m \cdot g \cdot \left(\frac{L_2 + H \cdot \gamma_x \pm T_1}{2} \pm R_1 \cdot \gamma_y \right), \tag{4.1}$$

$$Z_{2R,2L} = m \cdot g \cdot \left(\frac{L_1 - H \cdot \gamma_x \pm T_2}{2} \pm R_2 \cdot \gamma_y \right), \tag{4.2}$$

where index 1 refers to the front wheels/axle, index 2 – to the rear ones, R – right, L – left, L_1, L_2 – the distances between the vehicle's front and rear axle and its center of mass divided by the wheelbase, dimensionless, i.e., $L_1 = l_1/l_{12}$, $L_2 = \frac{l_2}{l_{12}}$, H – the vehicle center of mass over a road divided by the wheelbase (dimensionless), i.e., $H = \frac{h}{l_{12}}$ R_1, R_2 – parameters describing the front and rear suspensions (dimensionless) and, T_1, T_2 – parameters describing the vehicle's asymmetrical mass distribution (dimensionless); the unitary forces in the lateral direction are described by the given formulas (with index notations – as explained earlier) – see [23]:

$$\mu_{y1R,y1L} = \frac{\gamma_y \cdot L_2}{L_2 + H \cdot \gamma_x}, \tag{4.3}$$

$$\mu_{y2R,y2L} = \frac{\gamma_y \cdot L_1}{L_1 - H \cdot \gamma_x}. \tag{4.4}$$

The unitary forces in the longitudinal and lateral directions must satisfy the condition described by the following equation:

$$\left(\frac{\mu_x}{\mu_{\mathrm{MX}}}\right)^2 + \left(\frac{\mu_y}{\mu_{\mathrm{MY}}}\right)^2 \leq 1, \tag{4.5}$$

and none of the wheels lose contact with the road (i.e., normal forces cannot be less than zero). If these conditions are not fulfilled, the ABS will be activated and braking forces will be reduced. The algorithm for calculating the maximum intensity of braking on the road arc is shown in Fig. 2.

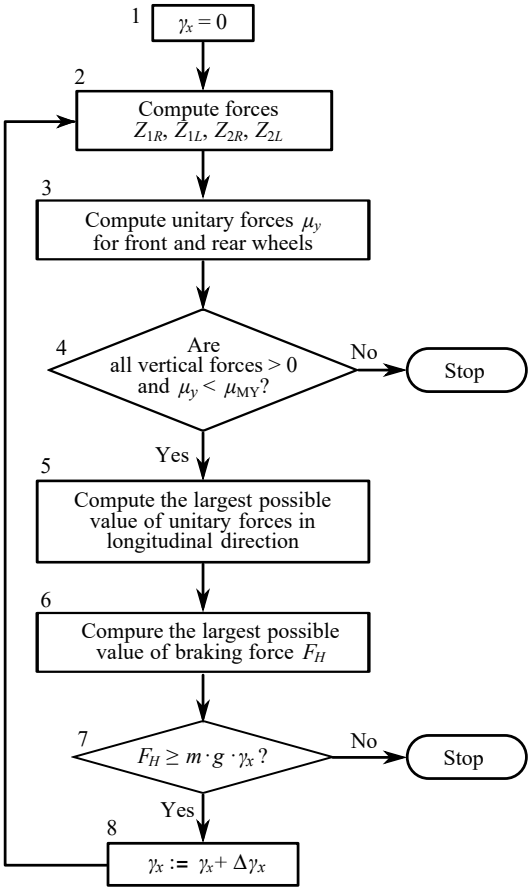

FIG. 2. Algorithm for computing the highest value of the braking intensity.

The initial value of the braking intensity is $\gamma_x = 0$ (block "1"). In the next step (block "2"), the vertical forces Z_{1R}, Z_{1L}, Z_{2R}, and Z_{2L} are computed. Using the braking intensity γ_x, the unitary forces in the lateral direction are computed (block "3"). In block "4", the following conditions are checked:

– the non-zero vertical forces between the tyres and the road:

$$Z_{1R}(\gamma_x, \gamma_y) > 0, \quad Z_{1L}(\gamma_x, \gamma_y) > 0, \quad Z_{2R}(\gamma_x, \gamma_y) > 0, \quad Z_{2L}(\gamma_x, \gamma_y) > 0,$$

– the lateral adhesion coefficients must not exceed their maximum limits:

$$\mu_{y1} \leq \mu_{\mathrm{MY}}, \qquad \mu_{y2} \leq \mu_{\mathrm{MY}}.$$

For the computed values of unitary lateral forces in each iteration, the largest possible values of the unitary longitudinal forces are calculated, according to the equation (block "5"):

$$\left(\frac{\mu_x}{\mu_{\mathrm{MX}}}\right)^2 + \left(\frac{\mu_y}{\mu_{\mathrm{MY}}}\right)^2 = 1 \rightarrow \mu_x = \mu_{\mathrm{MX}} \cdot \sqrt{1 - \left(\frac{\mu_y}{\mu_{\mathrm{MY}}}\right)^2}. \tag{4.6}$$

Now, in block "6", when the vertical forces between the tyres and the road surface and the largest values of the unitary longitudinal forces are determined, the braking force is computed as:

$$F_H = Z_{1R} \cdot \mu_{1R} + Z_{1L} \cdot \mu_{1L} + Z_{2R} \cdot \mu_{2R} + Z_{2L} \cdot \mu_{2L}. \tag{4.7}$$

This is the largest value of the braking force when the vehicle is turning with lateral intensity γ_y. If this force is not lower than the required force for braking with intensity γ_x, the next step of iteration is executed. This condition is checked in block "7". In block "8", the value of the braking intensity is updated for the next iteration.

If the condition in block "7" is not fulfilled, the calculations are stopped, and the current value of the braking intensity is considered the maximum braking intensity under the given conditions.

When a vehicle is braking with an ABS, 75% of the adhesion coefficient can be used. This is evident and due to the fundamental principle of ABS operation: when the maximum values of the unitary longitudinal forces between the tyres and the road are achieved and one or more wheels tend to lock, the braking force is modulated. As a result, the "effective values" of the unitary longitudinal forces are lower than the maximum values resulting from adhesion.

5. Determining the parameters of a vehicle (data for calculations)

There are some parameters in Eqs. (4.1) and (4.2): the parameters describing the location of the center of gravity: (L_1, L_2, H, T_1, T_2) and the parameters

describing the suspension of a vehicle: (R_1, R_2). Experimental measurements were conducted in the Institute of Vehicles at Warsaw University of Technology, which aimed to determine these parameters. A well-known method was used to find the height of the center of gravity – measuring the normal forces under the wheels of a vehicle standing horizontally on level ground, and then after lifting one of the axles (Fig. 3).

FIG. 3. Measurement of normal forces under the front axle wheels after lifting the front axle about 0.5 m.

Tests were carried out for several vehicles. Further are depicted the results for Opel Astra without a load:

1) vehicle on a level plane:
   - normal forces under front wheels: $Z_1 = 6150$ N,
   - normal forces under rear wheels: $Z_2 = 4340$ N,
   - normal forces under right wheels: $Z_P = 5180$ N,

   from calculations:

$$L_1 = 0.414, \qquad L_2 = 0.586,$$
$$T_1 = 6.84 \cdot 10^{-3}, \qquad T_2 = -30.11 \cdot 10^{-3};$$

2) front axle of the vehicle is lifted to $w = 0.58$ m:
   - normal forces under the rear wheels: $Z_2 = 4710$ N,

   finally, the height of the center of gravity was determined as:

$$h = 0.66 \text{ m} \rightarrow H = 0.26.$$

For accident reconstruction, it is necessary to perform calculations for a loaded vehicle. The conducted analysis shows that the distribution of passengers influences the load of the individual wheels. The results of the calculations are

presented in Table 1. The location of the driver and front seat passenger depends on the seat adjustment, therefore a range of distances is adopted.

TABLE 1. Influence of driver and passenger weight on the normal load of vehicle wheels.

Load (each person – 85 kg)	Occupant parameters and resulting wheel load changes						
	y [m]	x [m]	h [m]	ΔZ_{1R} [N]	ΔZ_{1L} [N]	ΔZ_{2R} [N]	ΔZ_{2L} [N]
Driver	0.65	−1.25–1.40	0.65	21	390	22	417
Passenger – front	−0.65	−1.25–1.40	0.65	390	21	417	22
Passenger – rear left	0.60	−2.20	0.70	9	98	64	679
Passenger – rear right	−0.60	−2.20	0.70	98	9	679	64

The center of gravity locations for the driver and front passenger were calculated based on seats geometry and their location analysis inside the vehicle. They are presented in Table 1 in the columns y, x, and h. The following symbols are used here: y – location relative to the longitudinal axis of the vehicle (positive values – position to the left), x – location relative to the front axle of the vehicle (positive values – in front), h – vertical position above the road surface.

The change in location of either the driver or the passenger in the front seats, each weighing 85 kg, significantly influences the normal loads on the wheels. Extreme cases of asymmetric loading of the vehicle were analyzed:

1) for the longitudinal displacement of the center of gravity:
   a) driver + four passengers:
   $$L_{1-\text{load5}} = 0.504, \qquad L_{2-\text{load5}} = 0.496, \qquad H_{\text{load5}} = 0.263,$$
   b) only driver:
   $$L_{1-\text{driv}} = 0.423, \qquad L_{2-\text{driv}} = 0.577, \qquad H_{\text{driv}} = 0.260;$$
2) for the asymmetrical loading of the vehicle:
   a) driver + passenger on rear left seat:
   $$T_1 = -3.34 \cdot 10^{-2}, \qquad T_2 = -1.09 \cdot 10^{-2},$$
   b) driver + passengers on front right and rear right seats:
   $$T_1 = 1.40 \cdot 10^{-2}, \qquad T_2 = 2.46 \cdot 10^{-2}.$$

The aim of the next measurement was to determine the values of R_1 and R_2. A lateral force was applied at a point located at height w, and the loads of the wheels were measured (Fig. 4).

The force F applied at the point located at height w changes the wheel loads in the same way as the lateral inertial force when the vehicle is moving along a curve with the intensity of turning defined as follows:

$$\gamma_y = \frac{F \cdot w}{m \cdot g \cdot H \cdot l_{12}}. \tag{5.1}$$

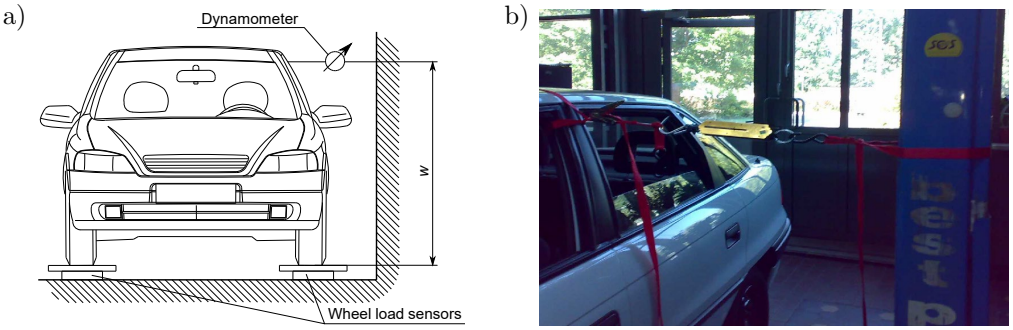

FIG. 4. Determination of the parameters R_1, R_2.

When a lateral force $F = 450$ N was applied, the values of the loads on the right front and the rear wheels were:

$$Z_{1P} = 2900 \text{ N}, \qquad Z_{2P} = 1800 \text{ N}.$$

Finally:

$$R_1 = -0.28, \qquad R_2 = -0.28.$$

6. Calculation example

In Fig. 5, there are presented the results of calculations of the stopping distance versus the radius of a road arc for initial vehicle velocities of 20 m/s, 25 m/s, and 30 m/s. The line marked "1D" corresponds to results obtained from the simple model, "3D" – the advanced model.

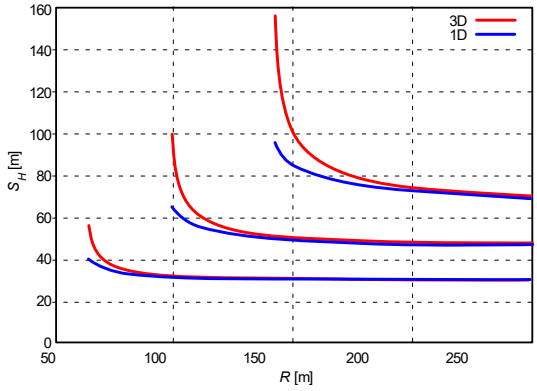

FIG. 5. Results of the calculations for a passenger car, the data of which was used for sample calculations.

The question is: when should the presented calculation scheme for stopping distance be applied necessarily, and when are the results similar to the results

for a straight road. Calculations were performed for a vehicle similar to the vehicle used in the above example (an average-class passenger car). The conclusion is that the difference between the length of the braking distances calculated using both methods is not higher than 10%, except when the vehicle is travelling on a curved road with a small radius close to the lateral adhesion limit. Calculations show that for a center of gravity location:

$$L_1 = 0.45\text{–}0.55, \quad H = 0.25\text{–}0.30$$

on an asphalt road ($\mu = 0.7$), the calculation error does not exceed 5% on the road arc where the initial lateral acceleration does not exceed 3 m/s^2, and below 10% – on the arc, where the initial lateral acceleration does not exceed 4 m/s^2 (Fig. 6). Based on these analyses, the maximum value of the road curve radius for the analyzed vehicle, below which the advanced model should be applied,

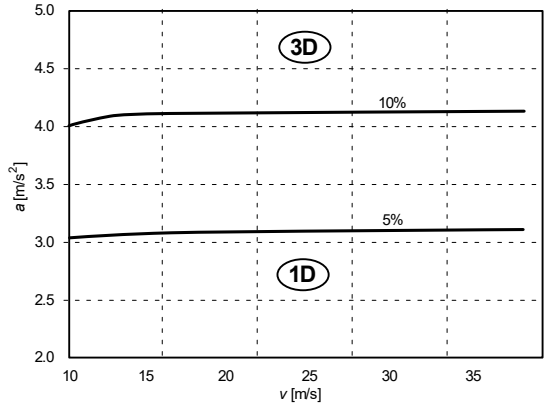

FIG. 6. Limits for applying the advanced braking distance model.

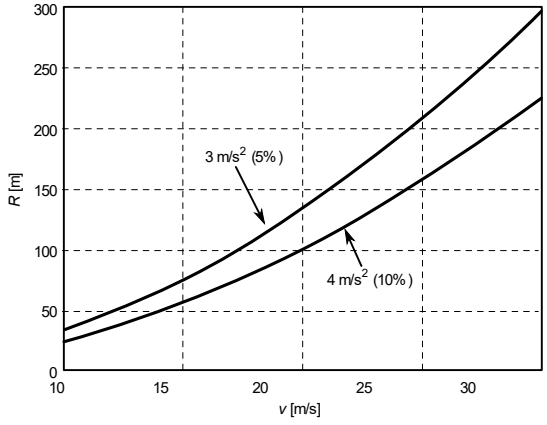

FIG. 7. Maximum radius of the curvature of the vehicle trajectory below which the advanced model should be applied.

is depicted in Fig. 7. The presented results apply to the majority of passenger cars used in Europe.

7. Conclusions

As the continuation of the issues discussed in the previous papers [28, 32], this paper extended the analysis of the braking process on the road arc. This analysis is important and may be useful in traffic incidents reconstruction.

One of the original issues presented in this article is the fact that the authors applied some dimensionless parameters to describe vehicle load state during braking.

Stopping distances on the road arcs can be significantly longer than on straight roads. When initial lateral acceleration on the road arcs is 3 m/s^2–4 m/s^2 or more, the stopping distance must be calculated using the advanced breaking model described in the article. When initial acceleration does not exceed these values, the difference between the length of the braking distance of the simple and advanced model does not exceed 5%–10%.

Determining the minimum length of the braking distance is one of the most frequently solved problems when, for example, investigating the cause of road accidents. In most cases, this is not a complicated calculation. In the case of a vehicle motion on a curved track, the issue becomes more complicated. The vehicle velocity decreases during braking and if the radius of the curvature (arc) remains constant, its lateral acceleration also decreases, since lateral acceleration depends on the vehicle's velocity. This allows for an increase in deceleration during braking. Of course, not every driver can brake optimally. However, driver assistance systems help achieve braking parameters close to optimal ones.

Variable lateral forces acting on a vehicle braking on a curve cause the radius of the vehicle's track to change during this maneuver. In practice, a driver can continuously correct the radius of their vehicle's track. The analysis in this paper assumed a constant radius of a vehicle track. However, it should be noted that most simulation programs applied in reconstruction of traffic incidents use a computational model of a vehicle in which the radius may change due to the action of lateral forces. The applied algorithms ensure that the track radius is approximately constant; however, some fluctuations in the radius are visible. They may cause the braking distance determined by the simulation program and the braking distance determined in the manner described in this paper to differ from each other.

A dimensionless approach to parameters related to suspension, vehicle mass distribution, and tangential forces between the tyre and the road may be useful especially if there is a need to perform comparative analyses, often necessary in traffic incident reconstruction.

References

1. Jurecki R.S., Stańczyk T.L., Modelling driver's behaviour while avoiding obstacles, *Applied Sciences*, **13**(1): 616, 2023, https://doi.org/10.3390/app13010616.

2. Jurecki R.S., Stańczyk T.L., Jaśkiewicz M.J., Driver's reaction time in a simulated, complex road incident, *Transport*, **32**(1): 44–54, 2017, https://doi.org/10.3846/16484142.2014.913535.

3. Jurecki R.S., Jaśkiewicz M.J., Guzek M., Lozia Z., Zdanowicz P., Driver's reaction time under emergency braking a car – Research in a driving simulatory, *Eksploatacja i Niezawodność – Maintenance and Reliability*, **14**(4): 295–301, 2012.

4. Xu J., Li L., Zhao R., Deng F., Li G., A Rapid verification system for automatic emergency braking control algorithm of passenger car, *Applied Sciences*, **13**(1): 508, 2023, https://doi.org/10.3390/app13010508.

5. Fildes B., Keall M., Bos N., Page Y., Pastor C., Pennisi L., Effectiveness of low speed autonomous emergency braking in real-world rear-end crashes, *Accident Analysis and Prevention*, **81**: 24–29, 2015, https://doi.org/10.1016/j.aap.2015.03.029.

6. Bauder M., Paula D., Pfeilschifter C., Petermeier F., Kubjatko T., Riener A., Schweiger H.-G., Influences of vehicle communication on human driving reactions: A simulator study on reaction times and behavior for forensic accident analysis, *Sensors*, **24**(14): 4481, 2024, https://doi.org/10.3390/s24144481.

7. Chen W., Li A., Jiang H., Risk assessment of roundabout scenarios in virtual testing based on an improved driving safety field, *Sensors*, **24**(17): 5539, 2024, https://doi.org/10.3390/s24175539.

8. Kim J., Jo K., Lim W., Lee M., Sunwoo M., Curvilinear-coordinate-based object and situation assessment for highly automated vehicles, *IEEE Transactions on Intelligent Transportation Systems*, **16**(3): 1559–1575, 2015, https://doi.org/10.1109/TITS.2014.2369737.

9. Roshan A., Abdelrahman M., Influence of aggregate properties on skid resistance of pavement surface treatments, *Coatings*, **14**(8): 1037, 2024, https://doi.org/10.3390/coatings14081037.

10. Yu M., Wu G., Kong L., Tang Y., Tire-pavement friction characteristics with elastic properties of asphalt pavements, *Applied Sciences*, **7**(11): 1123, 2017, https://doi.org/10.3390/app7111123.

11. Luo H., Chen S., Zhu L., Liu X., Zheng Y., Zhao R., Huang X., Investigation of surface textures deterioration on pavement skid-resistance using hysteresis friction models and numerical simulation method, *Friction*, **12**(4): 745–779, 2024, https://doi.org/10.1007/s40544-023-0811-1.

12. Ueckermann A., Wang D., Oeser M., Steinauer B., Calculation of skid resistance from texture measurements, *Journal of Traffic and Transportation Engineering (English Edition)*, **2**(1): 3–16, 2015, https://doi.org/10.1016/j.jtte.2015.01.001.

13. Dong D., Ye H., Luo W., Wen J., Huang D., Collision avoidance path planning and tracking control for autonomous vehicles based on model predictive control, *Sensors*, **24**(16): 5211, 2024, https://doi.org/10.3390/s24165211.

14. Xin T., Xu J., A data- and model-integrated driven method for recommending the maximum safe braking deceleration rates for trucks on horizontal curves, *Applied Sciences*, **14**(20): 9357, 2024, https://doi.org/10.3390/app14209357.

15. Zhu G., Hong W., Efficient nonlinear model predictive path tracking control for autonomous vehicle: Investigating the effects of vehicle dynamics stiffness, *Machines*, **12**(10): 742, 2024, https://doi.org/10.3390/machines12100742.

16. Hu D., Zhao J., Zheng J., Liu H., An adaptive cruise control strategy for intelligent vehicles based on hierarchical control, *World Electric Vehicle Journal*, **15**(11): 529, 2024, https://doi.org/10.3390/wevj15110529.

17. Májer J., Fodor D., Panyi P., Nagy F.T., Németh B.I., Enhancing safety-critical brake system testing with vector SIL over complex vector HIL, *Engineering Proceedings*, **79**(1): 34, 2024, https://doi.org/10.3390/engproc2024079034.

18. Skuza A., Szumska E.M., Jurecki R., Pawelec A., Modeling the impact of traffic parameters on electric vehicle energy consumption, *Energies*, **17**(21): 5423, 2024, https://doi.org/10.3390/en17215423.

19. Lai F., Liu J., Hu Y., An automatic emergency braking control method for improving ride comfort, *World Electric Vehicle Journal*, **15**(6): 259, 2024, https://doi.org/10.3390/wevj15060259.

20. Akhmedov D., Riskaliev D., Modeling of full vehicle dynamics for enhanced stability control, *Archives of Automotive Engineering – Archiwum Motoryzacji*, **105**(3): 88–102, 2024, https://doi.org/10.14669/AM/192666.

21. Kovalchuk S., Goryk O., Burlaka O., Kelemesh A., Evaluation of the strength of the truck tractor's frame under emergency braking conditions, *Archives of Automotive Engineering – Archiwum Motoryzacji*, **105**(3): 74–87, 2024, https://doi.org/10.14669/AM/192345.

22. Radzajewski P., Guzek M., Assessment of the impact of selected parameters of tractor-semitrailer set on the braking safety indicators, *Applied Sciences*, **13**(9): 5336, 2023, https://doi.org/10.3390/app13095336.

23. Kończykowski W., *Reconstruction and Analysis of the Course of a Road Accident* [in Polish: *Odtwarzanie i Analiza Przebiegu Wypadku Drogowego*], Stowarzyszenie Rzeczoznawców Techniki Samochodowej i Ruchu Drogowego, Paris–Warsaw, 1993.

24. Kim J., Voltage-based braking controls for electric vehicles considering weather condition and road slope, *Applied Sciences*, **13**(24): 13311, 2023, https://doi.org/10.3390/app132413311.

25. Yu P., Sun Z., Xu H., Ren Y., Tan C., Design and analysis of brake-by-wire unit based on direct drive pump–valve cooperative, *Actuators*, **12**(9): 360, 2023, https://doi.org/10.3390/act12090360.

26. Wiercioński J., Reza A., *Road Accidents: A Handbook for Court Experts* [in Polish: *Wypadki drogowe. Vademecum biegłego sądowego*], Institute of Forensic Research Publishers, Kraków, 2006.

27. Prochowski L., Unarski J., Wach W., Wicher J., *Basics of Road Accident Reconstruction* [in Polish: *Podstawy Rekonstrukcji Wypadków Drogowych*], WKŁ, Warszawa, 2025.

28. Fundowicz P., Braking distance on the arc trajectory [in Polish: Droga hamowania na łuku drogi], *Zeszyty Naukowe Instytutu Pojazdów*, **77**(1): 103–110, 2010.

29. Li K., Cao J., Yu F., Nonlinear tire-road friction control based on tire model parameter identification, *International Journal of Automotive Technology*, **13**(7): 1077–1088, 2012.

30. Jazar R.N., *Vehicle Dynamics: Theory and Application*, Springer Science + Business Media, 2008.

31. Rajamani R., *Vehicle Dynamics and Control*, Springer Science + Business, LCC, 2012.

32. Fundowicz P., Braking the vehicle during the ride on the arc [in Polish: Hamowanie pojazdu dwuosiowego podczas jazdy na łuku], *Archives of Automotive Engineering – Archiwum Motoryzacji*, **46**(4): 307–318, 2009.

Received December 19, 2024; accepted version June 18, 2025.
Online first November 6, 2025.